

Biomimetic Method To Assemble Nanostructured Ag@ZnO on Cotton Fabrics: Application as Self-Cleaning Flexible Materials with Visible-Light Photocatalysis and Antibacterial Activities

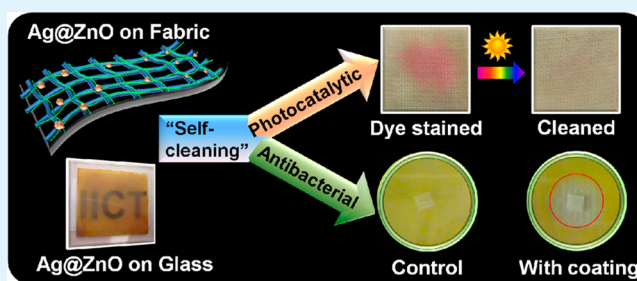
Joydeb Manna,[†] Srishti Goswami,[†] Nagaraju Shilpa,[†] Nivedita Sahu,[‡] and Rohit K. Rana^{*,†}

[†]Nanomaterials Laboratory, Inorganic and Physical Chemistry Division, and [‡]Biotechnology Laboratory, Medicinal Chemistry and Pharmacology, CSIR–Indian Institute of Chemical Technology, Uppal Road, Tarnaka, Hyderabad 500007, India

S Supporting Information

ABSTRACT: A bioinspired mineralization route to prepare self-cleaning cotton fabrics by functionalizing their surface with nanostructured Ag@ZnO is demonstrated herein. In a polyamine-mediated mineralization process, while the nucleation, organization and coating of ZnO is done directly from water-soluble zinc salts under mild conditions, the entrapped polyamine in the ZnO matrix acts as reducing agent to generate Ag(0) from Ag(I) at room temperature. The Ag@ZnO coated cotton fabrics are characterized by FESEM, HRTEM, XRD, and UV–vis–DRS to confirm the formation and coating of Ag@ZnO particles on individual threads of the fabric. The presence of Ag nanoparticles not only enables the ZnO-coated fabrics exhibiting improved photocatalytic property but also allows for visible-light-driven activities. Furthermore, it exhibits efficient antimicrobial activity against both Gram-positive and Gram-negative bacteria. Therefore, besides these multifunctional properties, the polyamine-mediated bioinspired approach is expected to pave way for functionalization of flexible substrates under mild conditions as desirable for the development and fabrication of smart, lightweight, and wearable devices for various niche applications.

KEYWORDS: biomimetics, flexible electronics, functional coatings, photocatalysis, ZnO nanostructures



INTRODUCTION

Zinc oxide, one of the most important II–VI semiconductor materials, has attracted immense research efforts for its application in photocatalysis.^{1–9} However, ZnO having its band gap in the UV region ($\lambda < 387$ nm) limits its application under solar irradiation, which comprises 43% visible light and 4% ultraviolet light.¹⁰ It is therefore desirable to tune the photoinduced activity to visible region by appropriate functionalization of ZnO in order to enable visible-light-driven activities. Many efforts have been made to obtain visible-light catalyst consisting engineered ZnO.^{11,12} One of the best methods is to have metal/ZnO heterostructure, where the surface plasmon resonance of metal nanoparticles increases the visible-light absorption along with the improvement of reactivity by restricting the recombination of charge carriers.^{13–16}

One of the recent interests has been to grow these photocatalytic materials on flexible substrates such as fabrics, plastics, textiles, and papers for making flexible, lightweight smart devices.^{17,18} Particularly, coating of visible-light photocatalysts can afford self-cleaning fabrics. In this context, there have been few reports on visible-light-driven self-cleaning flexible materials. Wu et al. have shown that functionalization of cotton surfaces with N-TiO₂/AgI and TiO₂/Ag/AgCl particles can exert visible-light-induced properties toward the degrada-

tion of methyl orange.^{19,20} Similarly, Wang et al. have used Au/TiO₂/SiO₂ composites as photocatalyst on cotton fabrics and demonstrated the self-cleaning activities under visible-light.²¹ On the other hand, Porphyrin/TiO₂ based materials have been utilized by Afzal et al. for fabricating self-cleaning cotton fabric.²² Similarly, Khajavi et al. have demonstrated dicarboxylic acid/TiO₂-based self-cleaning cotton fabric.²³ However, thus-developed coating methods involve either presynthesis of the photocatalysts under harsh conditions such as acidic medium and high pressure and temperature or additional coating steps such as high-energy coating and drying processes. It is therefore essential that the nanostructured functional materials are grown directly on the substrate under benign conditions, as the harsh conditions such as elevated temperature, pressure, and extreme pH can decrease the stability of these substrates. The challenge is to develop a “green” method for the coating functional materials on flexible substrates like cotton fabric enabling sufficient interfacial adhesion, smooth coating, and stability.

Herein, we demonstrate that effective utilization of the polyamine-mediated bioinspired mineralization routes^{24,25} can lead to functionalization of cotton fabrics with nanostructured

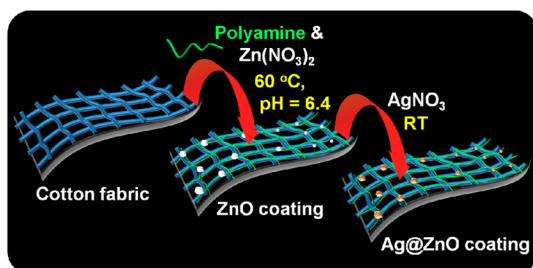
Received: January 21, 2015

Accepted: March 31, 2015

Published: March 31, 2015

Ag@ZnO suitable for developing self-cleaning flexible materials (Scheme 1). Particularly, we use poly(allylamine) for the

Scheme 1. Illustration of the Method Employed in Polyamine-Mediated Coating of ZnO and Ag@ZnO on Cotton Fabric



formation and coating of Ag@ZnO from a simple water-soluble zinc salt ($\text{Zn}(\text{NO}_3)_2$) under mild conditions. The polyamine while mineralizing ZnO on the cotton fabrics, further facilitates the reduction of Ag(I) to form Ag(0) without any use of external reducing agent. The method allows the functionalized coating to take place under benign conditions and results in a uniform coating on the fabric displaying multifunctional properties useful for visible-light-driven photocatalysis and antibacterial activities.

EXPERIMENTAL SECTION

Materials. Zinc nitrate hexahydrate ($\text{Zn}(\text{NO}_3)_2 \cdot 6\text{H}_2\text{O}$), Poly(allylamine) (PAA, 17 kDa) and Silver nitrate (AgNO_3) were procured from Sigma-Aldrich and used as received. The cotton fabrics were procured from local industry and cleaned with nonionic detergent. In all cases, Millipore water (18.2 M Ω) was used to prepare the solutions.

Preparation of ZnO Particles. The synthesis of nanostructured ZnO was done using PAA as the mineralizer under mild conditions based on the earlier report with little modification.²⁴ A required amount of 100 mg mL⁻¹ Poly(allylamine) solution was added to a 25 mL 0.1 M $\text{Zn}(\text{NO}_3)_2 \cdot 6\text{H}_2\text{O}$ aqueous solution to get a final PAA concentration of 2 mg mL⁻¹. The resulted mixture was kept at a temperature maintained at 60 °C for a period of 2 h. The white colloids were then separated by centrifugation, washed twice with Millipore water, and dried at room temperature.

Preparation of Ag@ZnO Particles. For synthesis of Ag@ZnO particles, freshly prepared ZnO spheres were dispersed in 55 mL of water followed by addition of a AgNO_3 solution and stirred for 24 h. The concentration of the AgNO_3 solution was varied to have different amount of silver loading and the corresponding samples were named as Ag@ZnO-P1, Ag@ZnO-P2.5, and Ag@ZnO-P5 for AgNO_3 concentration 1×10^{-5} M, 2.5×10^{-5} M, and 5×10^{-5} M, respectively. With time, the white-colored ZnO became light yellow as Ag nanoparticles deposited on ZnO. The reduction of Ag(I) to Ag(0) occurred because of the polyamine present in the ZnO matrix without addition of any external reducing agent. Finally, the as-synthesized Ag@ZnO particles were washed thrice with Millipore water and dried at room temperature.

Preparation of ZnO coated cotton fabrics (ZnO@CF). A cotton fabric (22 threads/cm²) was immersed in an aqueous solution containing 2 mg mL⁻¹ PAA and 0.1 M $\text{Zn}(\text{NO}_3)_2 \cdot 6\text{H}_2\text{O}$, which was then kept at 60 °C for a period of 1 h for in situ coating of ZnO on the fabric. Thus, coated cotton fabric was washed thrice with Millipore water and dried at room temperature.

Preparation of Ag@ZnO-Coated Cotton Fabrics (Ag@ZnO@CF). For the preparation of Ag@ZnO-coated cotton fabrics, a freshly prepared ZnO coated cotton fabric was dipped in a AgNO_3 solution and stirred overnight. The concentration of the AgNO_3 solution was varied to load different amount of silver and the corresponding

samples were named as Ag@ZnO@CF-1, Ag@ZnO@CF-2.5, and Ag@ZnO@CF-5 for AgNO_3 concentration 1×10^{-5} M, 2.5×10^{-5} M, and 5×10^{-5} M, respectively. With time, the white color ZnO-coated cotton fabric became light yellow as Ag nanoparticles were formed. Finally, the as-synthesized Ag@ZnO-coated cotton fabric was washed thrice with Millipore water and dried at room temperature.

Measurement of Photocatalytic Activity of Ag@ZnO Particles. The photocatalytic activity of the prepared Ag@ZnO particles were investigated in degradation of rhodamine B (RhB) in an aqueous solution at room temperature under visible light ($\lambda > 400$ nm, 400 W) irradiation. The experimental details were as follows: 5 mg of the as prepared catalyst was dispersed in 5 mL of 0.01 mM RhB aqueous solution in the reactor vessel. Before irradiation the solution was magnetically stirred in the dark for about 30 min to ensure the establishment of adsorption–desorption equilibrium of the dye on the catalyst surface. The resulted reaction mixture was then exposed to visible light ($\lambda > 400$ nm, 400 W) in a photocatalytic reactor setup for a certain time period and then the catalyst was removed from the unreacted rhodamine solution by centrifugation. Reaction progress was monitored by measuring the decrease in concentration of RhB using UV–vis spectrophotometer. A blank experiment was carried out without using the catalyst. ZnO particles were also tested for any catalytic activities.

Measurement of Photocatalytic Activity of Coated Fabrics. The experimental details were as follows: A 1.5×1.5 cm² Ag@ZnO-coated cotton fabric was placed in 3 mL of 0.01 mM RhB aqueous solution in a test tube. Before irradiation, the solution was magnetically stirred in the dark for about 30 min to ensure the establishment of adsorption–desorption equilibrium of the dye on the catalyst surface. The resulted reaction mixture was then exposed to visible light ($\lambda > 400$ nm, 400 W) in a photocatalytic reactor setup for a certain time period and then the cotton fabric was removed from the unreacted rhodamine solution. The photoassisted decrease in concentration of RhB was determined by UV–vis spectrophotometer. Uncoated (UCF) and ZnO-coated cotton fabrics were also tested for any catalytic activities.

Photocatalytic Activity under Solar Light. The photocatalytic activities of the Ag@ZnO coated cotton fabrics under solar light were performed by exposing a dye stained cotton fabric under Sunlight. For this, a portion of Ag@ZnO@CF-2.5 sample was stained with a concentrated RhB solution and exposed directly to sunlight for few hours.

Antibacterial Activities of the Coated Fabrics. The antibacterial properties of the coated-fabrics were examined against both the Gram-positive bacteria strain (*Staphylococcus aureus*) and the Gram-negative strain (*Pseudomonas Aeruginosa*). The above bacterial strains were cultured overnight for their growth in Nutrient Broth (NB) medium with required aeration at 37 °C. It was then transferred into a fresh NB medium on the next day having 0.1 OD (optical density) at a wavelength of 600 nm. After the culture was reached to ~0.3 OD at the same wavelength, the cells were centrifuged followed by washing two times with 0.9% NaCl solution at pH 7. Then a piece of (1 cm²) of UCF (uncoated cotton fabric as reference material), ZnO@CF and Ag@ZnO@CF were placed into a vial having 4.5 mL of 0.9% NaCl solution. Then, the previously washed and diluted cells were pipetted (500 μL) to the vial. The starting bacterial amount in the vial was about 1×10^7 CFU/mL. A 0.9% NaCl solution without any cotton fabric was also included in the experiment as another control to make sure that the reduction in the amount of bacteria was as a result of ZnO@CF and Ag@ZnO@CF. The above bacterial suspensions were then incubated at 170 rpm and 37 °C for a time up to 4 h. A 100 μL sample from each vial was taken out at the start and after each interval of 1 h. The growth of bacteria was then evaluated by monitoring the optical density (OD₆₀₀) at different times using a spectrometer (microplate reader TECAN M200). Further evaluation was done to find the rate of inhibition (%) as per $([\text{OA}]^i - [\text{OA}]^t) / [\text{OA}]^i$, where $[\text{OA}]^i$ = initial optical absorption of the bacteria (untreated) and $[\text{OA}]^t$ = optical absorption of the treated bacteria at time t .²⁶

Stability Test of Ag(0) Nanoparticles in the Coated Fabrics.

For the stability test of the coated Ag(0), the piece of coated cloth was placed in bacterial suspension and the bacterial suspension was withdrawn at every 1 h, separated from bacteria by centrifugation, and checked for Ag leaching using ICP-OES.

Characterizations. Powder XRD patterns were recorded on a Siemens (Cheshire, UK) D5000 X-ray Diffractometer by means of $\text{CuK}\alpha$ ($\lambda = 1.5406 \text{ \AA}$) radiation at 40 kV and 30 mA with a standard monochromator equipped with a Ni filter. The powder XRD patterns were used to identify the crystalline phases of the deposited ZnO and to estimate the crystallite size using the Debye–Scherrer formula [$L(hkl) = 0.9\lambda/\Delta(hkl)\cos\theta$], where λ is the X-ray wavelength, θ is the Bragg's angle, and Δ is the full width of the diffraction line (hkl) at half-maximum intensity. SEM analyses were performed by using a Hitachi S-3000N scanning electron microscope operated at 10 kV. Dynamic light scattering (DLS) characterizations were done by a Malvern Zetasizer Nano series (Nano ZS). TGA was performed with a TG/DTA 7200, EXSTAR under a N_2 atmosphere, with a heating rate of $10^\circ\text{C min}^{-1}$ from 25–800 $^\circ\text{C}$. Elemental analysis was carried out by inductively coupled plasma-optical emission spectroscopy, Thermo Elemental, IRIS Intrepid II XDL. The cotton samples were digested in concentrated HCl and submitted for elemental analysis. UV–vis–DRS were recorded on a UV–vis spectrophotometer Carry-5000.

RESULTS AND DISCUSSION

Fabrication of Ag@ZnO-Coated Cotton Fabric. To coat Ag@ZnO on cotton fabrics, as mentioned in the Experimental Section, in an in situ process, we first immersed the cotton fabric in a ZnO precursor solution with poly(allylamine) at 60 $^\circ\text{C}$. In the second step, when thus-coated fabric interacted with AgNO_3 solution, the initial white fabric gradually turned to yellow. It was a visual indication for the reduction of Ag(I) ions to form Ag(0). We observed a similar phenomenon for the ZnO spheres, which were obtained in absence of the fabric, to generate Ag@ZnO. The poly(allylamine) besides its role as mineralizer for the formation of nanostructured ZnO,²⁴ is also known to act as a reducing agent.^{27,28} Hence its presence in the ZnO matrix facilitates the reduction of Ag(I) ions to generate Ag(0) nanoparticles (Scheme 1).

The as-synthesized Ag@ZnO@CF samples were imaged under scanning electron microscopy (SEM) and transmission electron microscopy (TEM). SEM analysis showed the presence of nanostructured ZnO and Ag@ZnO with the particles sizes of 150–250 nm, coated uniformly on to individual threads in the fabric (Figure 1). As seen in the high-resolution images (Figure 1 and see the Supporting Information, Figure S1), the Ag@ZnO particles were nearly spherical in shape with a diameter range of 150–250 nm. The FESEM image taken with LABE (low-angle backscatter electron) detector shows the clear difference in contrast between ZnO and Ag nanoparticle as indicated by the red arrows in Figure 1h. The formed Ag nanoparticles were spherical in shape with a diameter of 12–19 nm (see the Supporting Information, Figure S1). From the HRTEM analysis, it was observed that each spherical particle was composed of many nanosized crystallites having a lattice spacing of 0.27 nm for ZnO and 0.23 nm for Ag nanoparticles (Figure 2).

The structural characterization of ZnO coated on the cotton fabric was carried out by powder XRD analyses. As shown in Figure S2 (see the Supporting Information), the XRD pattern could be indexed to a wurtzite phase of ZnO (JCPDS card No. 36–1451). The crystallite size of ZnO was estimated from Debye–Scherrer formula to be 11 nm. As per the proposed mechanism the amine groups of poly(allylamine) coordinate to

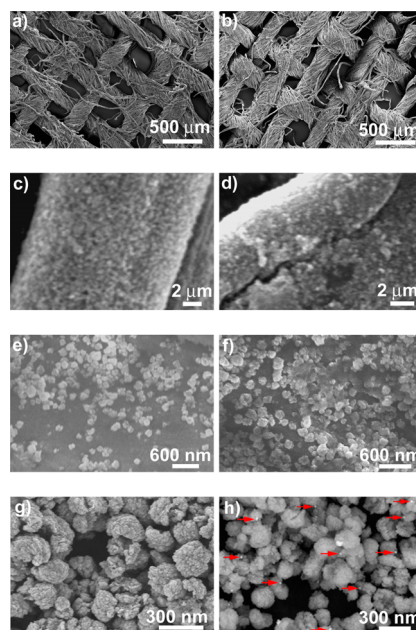


Figure 1. SEM images taken at different magnifications for the cotton fabrics (a, c, e) ZnO@CF and (b, d, f) Ag@ZnO@CF-2.5; FESEM images depicting (g) ZnO and (h) Ag@ZnO particles. The red arrows indicate the Ag nanoparticles.

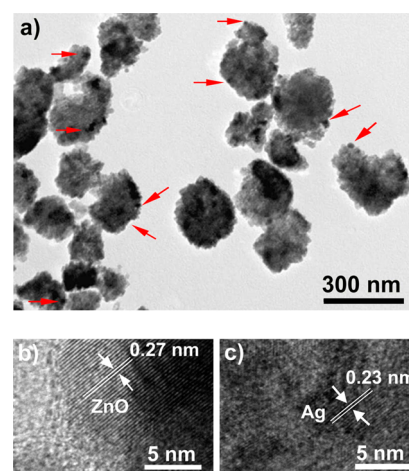


Figure 2. TEM showing (a) Ag@ZnO particles; lattice fringes of (b) ZnO and (c) Ag particles. The red arrows indicate the Ag nanoparticles.

Zn(II) ions to form zinc/amine complex, which upon heating at 60 $^\circ\text{C}$ generates ZnO nanostructures.²⁴ Further, the role of poly(allylamine) in the reduction of Ag(I) to Ag(0) was monitored by the UV–vis spectroscopic measurements. The formation of Ag(0) nanoparticles was confirmed by its typical surface plasmon resonance centered at 420 nm (Figures 3a, 3b), whereas an absorbance onset at 391 nm indicated ZnO, corresponding to a band gap of 3.17 eV. As reported earlier, the poly(allylamine) is therefore responsible for the reduction of Ag(I) to Ag(0) as well.²⁸ The morphological and structural analyses together indicated that the polyamine-mediated synthesis of Ag@ZnO was successful in coating these materials on to the cotton fabric.

The amount of ZnO loaded on the lining cloth was 1.01% as found by elemental analysis (ICP-OES). The corresponding Ag loadings in the fabric were 0.012, 0.019, and 0.027% for the

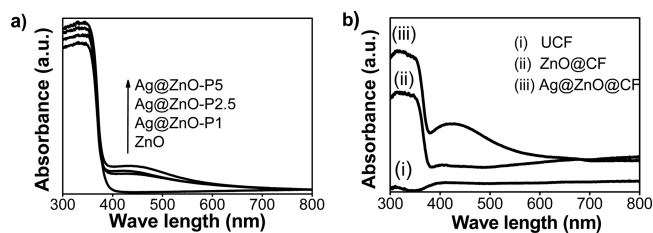


Figure 3. UV-vis-DRS of (a) ZnO and different Ag-loaded Ag@ZnO particles and (b) cotton fabric samples (i) UCF, (ii) ZnO@CF, and (iii) Ag@ZnO@CF-2.5.

samples Ag@ZnO@CF-1, Ag@ZnO@CF-2.5, and Ag@ZnO@CF-5, respectively. In the case of Ag@ZnO prepared without the fabric, the Ag loadings were 0.04, 0.10, and 0.15% for the samples Ag@ZnO-1, Ag@ZnO-2.5, and Ag@ZnO-5, respectively. The Ag loading in the case of the fabric (Ag@ZnO@CF) was less than that of without fabric (Ag@ZnO). This indicates that the attachment of PAA-ZnO particles with the fabric restricts the AgNO₃ to interact only through the exposed surface of these particles. In the later case, the PAA-ZnO particles are in colloidal form which allows the whole surface to be accessible by AgNO₃ to interact with PAA, thereby leading to more amount of Ag(0) being formed. As obtained from dynamic light scattering measurements, the average hydrodynamic size of the particles increased from 220 nm for only ZnO spheres to 258, 282, and 295 nm for Ag@ZnO-1, Ag@ZnO-2.5, and Ag@ZnO-5, respectively (see the Supporting Information, Figure S3). This indicates that the particle size increased with an increase in Ag loading.

To ascertain the presence of polyamine and to follow the steps involved in the coating process, we tagged polyamine with a fluorescent molecule (fluorescein isothiocyanate, FITC). The FITC-tagged polyamine (FITC-polyamine) was then used for the coating of ZnO and Ag@ZnO onto the cotton fabric and imaged under a fluorescence microscope (Figure 4). As shown in Figure 4c, d, the coating of ZnO onto the fabrics resulted in green fluorescent colored threads, whereas the control

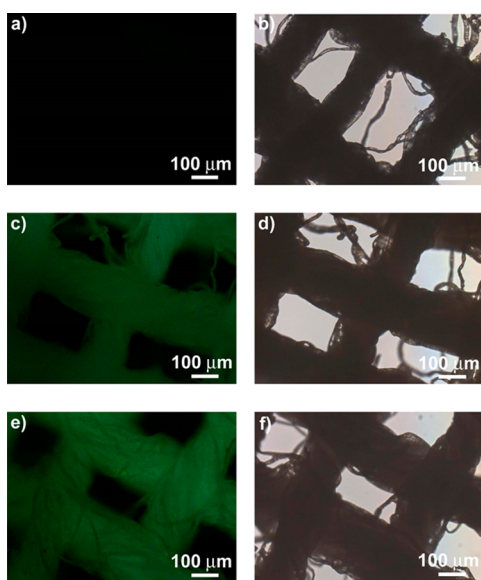


Figure 4. Fluorescence microscopic images of (a, b) UCF, (c, d) ZnO@CF, and (e, f) Ag@ZnO@CF in green and bright field, respectively. The coating was performed using FITC-polyamine.

experiment with uncoated cotton fabric (UCF) did not show any fluorescence (Figure 4a, b). Moreover, the Ag@ZnO-coated sample also showed (Figure 4e, f) the fluorescent green color along the threads. This indicated that the polyamine was also bound to the fabric threads during the coating process and the entrapped polyamine was available to reduce the Ag(I) to Ag(0). Even after several washings, the coated polyamine and Ag@ZnO remained stable, as observed from fluorescence microscopy and elemental analysis.

The Ag@ZnO-coated cotton fabrics were further characterized by X-ray photoelectron spectroscopy (XPS) (see the Supporting Information, Figure S4). In the case of Ag@ZnO@CF-2.5, the binding energies for Zn 2p were 1020.7 and 1044 eV, corresponding to Zn 2p_{3/2} and Zn 2p_{1/2}, respectively. The other binding energies 531.4, 398.6, and 283.8 eV correspond to O 1s, N 1s, and C 1s, respectively, because of the entrapped polyamine and cotton fabric.^{29,30} The presence of Ag(0) was evidenced from the binding energies seen at 366.6 and 372.8 eV, corresponding to Ag 3d_{5/2} and Ag 3d_{3/2}, respectively.³¹ Similar observations were made for the Ag@ZnO particles prepared in the absence of cotton fabric (see the Supporting Information, Figure S4). The TG-DTA analysis showed a weight loss of around 80% in the temperature range of 300–600 °C for both the ZnO and Ag@ZnO-coated fabrics (see the Supporting Information, Figure S5). This weight loss corresponds to the decomposition of both polyamine and the cotton cellulose.

Photocatalysis Studies. The photoinduced catalytic efficiency of different Ag@ZnO particles as well as the ZnO- and Ag@ZnO-coated cotton fabrics were investigated using the degradation of the rhodamine B dye, which was used as a model contaminant. Photocatalytic activities were monitored by measuring the change in UV-vis absorbance at 553 nm for the unreacted dyes over time, as shown in Figure 5a, c. It was found that among the three catalysts prepared with different Ag contents, the sample Ag@ZnO-P2.5 had the best activity, which degraded the RhB within 1.5 h under the illumination of visible light (Figure 5b), suggesting an optimum and well-dispersed Ag

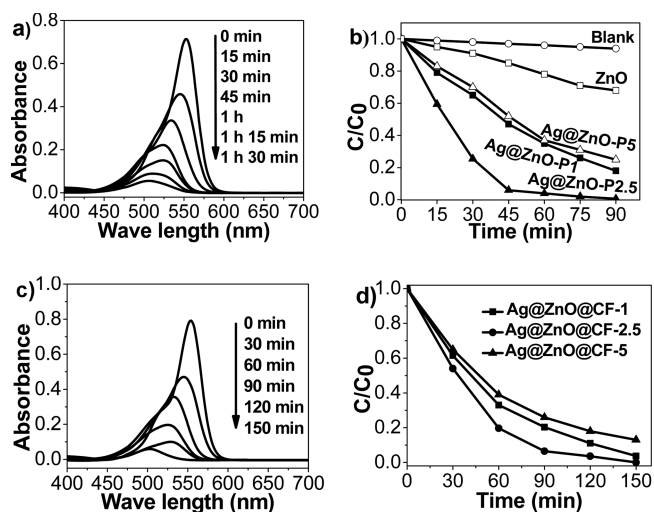


Figure 5. (a) UV-vis spectra of RhB present in the reaction mixture after irradiated with visible-light for different time duration over (a) Ag@ZnO-P2.5 and (c) Ag@ZnO@CF-2.5 sample. The change in RhB concentration as a function of visible-light irradiation time for different (b) Ag-loaded ZnO particles and (d) Ag@ZnO-coated cotton fabrics.

nanoparticles (see the Supporting Information, Table S1). In the case of coated cotton fabrics, the sample Ag@ZnO@CF-2.5 had the best activity, which degraded the RhB within 2.5 h under the illumination of visible light (Figure 5d and the Supporting Information, Figure S6).

The reusability of the catalyst was further checked by using the Ag@ZnO@CF-2.5 sample. For each cycle, the cotton sample was irradiated with visible light for various time periods and then the cotton fabric was removed from the unreacted rhodamine solution, washed thrice with Millipore water and then reused. We checked up to fifth cycles and it was observed that the coated cotton sample showed almost similar activities in each case (Figure 6). This suggests that the presence of

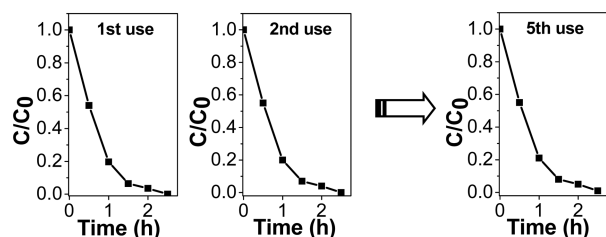


Figure 6. Reusability of the catalyst Ag@ZnO@CF-2.5 for RhB degradation under visible light for several cycles.

polyamine during the synthesis and coating on the fabric allows the catalytically active materials to be well adhered to the fabric and hence prevents any leaching during the reaction and as well as during the washing process. Furthermore, the self-cleaning properties of the Ag@ZnO coated cotton fabrics were tested under sunlight exposure. A portion of Ag@ZnO@CF-2.5 sample was stained with a concentrated RhB solution and exposed directly to sunlight for few hours (Figure 7a, b). It is observed that the color stain on the fabric could be completely removed after an exposure for 15 h. In contrast, for UCF the color of the stained RhB remained almost unchanged when exposed to sunlight for the same duration of time (see the Supporting Information, Figure S7).

Thus, developed coating methodology could be extended to functionalize other substrate like glass. Both the ZnO- and Ag@ZnO-coated glass showed a transparent thin layer of coating of the particles (Figures 7c, d). To check the self-cleaning properties of the Ag@ZnO-coated glass, it was stained with a concentrated RhB solution and exposed directly to sunlight (Figures 7c, d). It was observed that the color of the RhB disappeared after an exposure time of 10 h.

Antibacterial Studies. To evaluate the self-cleaning properties of the ZnO and Ag@ZnO coated cotton fabric, we used Gram-positive (*Staphylococcus aureus*) and Gram-negative (*Pseudomonas Aeruginosa*) bacteria. A $1 \times 1 \text{ cm}^2$ cotton piece of the ZnO@CF and Ag@ZnO@CF samples were placed with a bacterial culture in an agar medium (Muller–Hinton) following the Kirby–Bauer protocol for zone-of-inhibition testing. The zone-of-inhibition shown in Figure 8 and in the Supporting Information (Figures S8 and S9), indicates that the ZnO@CF and Ag@ZnO@CF samples efficiently inhibit the growth for both the bacteria and led to the zone development around the bandage. On the other hand, the UCF sample did not show any zone formation. The corresponding plot of diameter of zone of inhibition is shown in Figure 8b. The results showed that with the amount of Ag loading the antibacterial activity increased with 0.019 wt % being the optimum one.

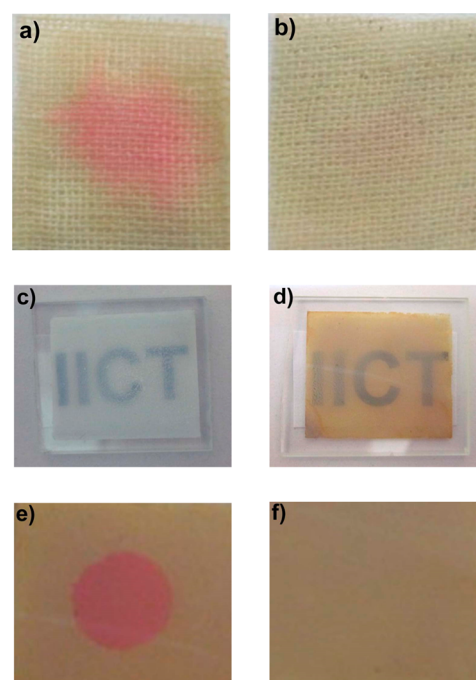


Figure 7. Photographs of the Ag@ZnO@CF-2.5 coated cotton fabrics stained with RhB dye (a) before and (b) after exposure to sunlight for 15 h; photographs of the (c) ZnO- and (d) Ag@ZnO-coated glass showing transparency; stained glass with RhB dye (e) before and (f) after exposure to sunlight for 10 h.

Further, the bacterial growth curves are also analyzed (Figure 8 and the Supporting Information, Figure S9). The OD (optical densities) was measured at a wavelength of 600 nm. Since at this wavelength the bacterial components do not interfere, the absorbance is only due to the turbidity variation as a result of variation in the number of cells. All the coated cotton fabrics show excellent antibacterial activities against both Gram –ve and Gram +ve bacteria. The sample Ag@ZnO@CF-2.5 and Ag@ZnO@CF-5 show a 100% reduction in viability for *S. Aureus* and *P. Aeruginosa* after 4 and 6 h, respectively (Figure 8 and the Supporting Information, Figure S9). The reduction in bacterial viabilities for all others cotton fabrics are shown in the Supporting Information, Table S2. In contrast, for the UCF sample, the growth curve remained almost similar to that of the original bacterial concentration. Thus, the ability for inhibiting bacteria was only due to the coated materials on the fabric.

To study the stability of the coated Ag(0) on to the cotton fabrics, we analyzed the bacterial medium for silver content at various time intervals (see the Experimental Section). We did not observe any silver leaching in the experimental duration up to 5 h, as it was below the detection limit of ICP analysis. However, when continued further, we could get only 0.01, 0.08, and 0.1 ppm of silver present in the medium after 24 h for Ag@ZnO@CF-1, Ag@ZnO@CF-2.5, and Ag@ZnO@CF-5, respectively. Although it is known that the silver in Ag(0) state is less prone to leaching because of its very slow oxidation,³² the polyamines in our case can further be responsible to keep the silver nanoparticles in the ZnO matrix attached with fabric. Although the exact antibacterial mechanism is still not fully known, the generation of reactive oxygen species (ROS) together with the slow silver leaching from Ag(0) in Ag@ZnO@CF may contribute to the activity.³³

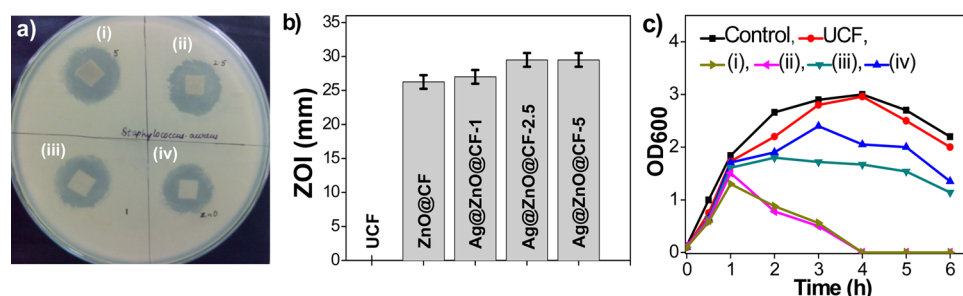


Figure 8. (a) Zone of inhibition, (b) bar diagram showing the ZOI (zone of inhibition), and (c) bacterial growth curve against *S. Aureus* in the presence of (i) Ag@ZnO@CF-5, (ii) Ag@ZnO@CF-2.5, (iii) Ag@ZnO@CF-1, and (iv) ZnO@CF.

CONCLUSIONS

It is demonstrated that the polyamine-mediated mineralization could be successfully utilized for the formation of Ag@ZnO and to uniformly coat Ag@ZnO on to the cotton fabric. The presence of polyamine not only helped in the formation of both ZnO and Ag nanomaterials, but also allowed efficient coating of these materials on to the fabric threads. The resulted materials were found to exhibit efficient photocatalytic activity and self-cleaning properties under visible light. It was effective against both Gram-positive and Gram-negative bacteria. The coated substrates were also efficient in removal of dye stains under sunlight exposure. The coating technique enabled other substrates like glass to be functionalized. Thus, the method affords an environmentally benign coating technique, which can further be explored to impart multifunctionalities on flexible substrates useful in diverse applications including flexible smart devices.

ASSOCIATED CONTENT

Supporting Information

Characterization data for SEM, XRD, DLS, XPS, and TG-DTA and results of photodegradation of RhB and antibacterial activities. This material is available free of charge via the Internet at <http://pubs.acs.org>.

AUTHOR INFORMATION

Corresponding Author

*E-mail: rkrana@iict.res.in. Fax: (+91) 4027-160-921.

Notes

The authors declare no competing financial interest.

ACKNOWLEDGMENTS

Financial support from the CSIR, India (IntelCoat CSC-0114 and NanoSHE BSC-0112); and the UGC, India (SRF) is greatly acknowledged. S.G. thanks IASc-INSA-NASI for Summer Research Fellowship-2012.

REFERENCES

- Huang, M. H.; Mao, S.; Feick, H.; Yan, H.; Wu, Y.; Kind, H.; Weber, E.; Russo, R.; Yang, P. D. Room-Temperature Ultraviolet Nanowire Nanolasers. *Science* **2001**, *292*, 1897–1898.
- Park, H.-K.; Lee, K. Y.; Seo, J.-S.; Jeong, J. A.; Kim, H.-K.; Choi, D.; Kim, S.-W. Charge-Generating Mode Control in High-Performance Transparent Flexible Piezoelectric Nanogenerators. *Adv. Funct. Mater.* **2011**, *21*, 1187–1193.
- Schwartz, V. B.; Th  tiot, F.; Ritz, S.; P  tz, S.; Choritz, L.; Lappas, A.; F  rch, R.; Landfester, K.; Jonas, U. Antibacterial Surface Coatings from Zinc Oxide Nanoparticles Embedded in Poly(*N*-isopropylacrylamide) Hydrogel Surface Layers. *Adv. Funct. Mater.* **2012**, *22*, 2376–2386.
- Lehr, D.; Luka, M.; Wagner, M. R.; Bulger, M.; Hoffmann, A.; Polarz, S. Band-Gap Engineering of Zinc Oxide Colloids via Lattice Substitution with Sulfur Leading to Materials with Advanced Properties for Optical Applications Like Full Inorganic UV Protection. *Chem. Mater.* **2012**, *24*, 1771–1778.
- Ra, H.-W.; Kim, J.-T.; Khan, R.; Sharma, D.; Yook, Y.-G.; Hahn, Y.-B.; Park, J.-H.; Kim, D.-G.; Im, Y.-H. Robust and Multifunctional Nanosheath for Chemical and Biological Nanodevices. *Nano Lett.* **2012**, *12*, 1891–1897.
- Beek, W. J. E.; Weink, M. M.; Janssen, R. A. J. Efficient Hybrid Solar Cells from Zinc Oxide Nanoparticles and a Conjugated Polymer. *Adv. Mater.* **2004**, *16*, 1009–1013.
- Aurang, P.; Demircioglu, O.; Es, F.; Turan, R.; Unalan, H. E. ZnO Nanorods as Antireflective Coatings for Industrial-Scale Single-Crystalline Silicon Solar Cells. *J. Am. Ceram. Soc.* **2013**, *96*, 1253–1257.
- Sinha, A. K.; Basu, M.; Pradhan, M.; Sarkar, S.; Pal, T. Fabrication of Large-Scale Hierarchical ZnO Hollow Spherulites for Hydrophobicity and Photocatalysis. *Chem.—Eur. J.* **2010**, *16*, 7865–7874.
- Shinde, V. R.; Gujar, T. P.; Noda, T.; Fujita, D.; Vinu, A.; Grandcolas, M.; Ye, J. Growth of Shape- and Size-Selective Zinc Oxide Nanorods by a Microwave Assisted Chemical Bath Deposition Method: Effect on Photocatalysis Properties. *Chem.—Eur. J.* **2010**, *16*, 10569–10575.
- Zou, Z. G.; Ye, J. H.; Sayama, K.; Arakawa, H. Direct Splitting of Water under Visible light Irradiation with an Oxide Semiconductor Photocatalyst. *Nature* **2001**, *414*, 625–627.
- Ahn, K. S.; Yan, Y.; Shet, S.; Deutsch, T.; Turner, J.; Al-Jassim, M. Enhanced Photoelectrochemical Responses of ZnO Films through Ga and N Codoping. *Appl. Phys. Lett.* **2007**, *91*, 231909.
- Yang, X.; Wolcott, A.; Wang, G.; Sobo, A.; Fitzmorris, R. C.; Qian, F.; Zhang, Z. J.; Li, Y. Nitrogen-doped ZnO Nanowire Array for Photoelectrochemical Water Splitting. *Nano Lett.* **2009**, *9*, 2331–2336.
- Jensen, T. R.; Malinsky, M. D.; Haynes, C. L.; Duyn, R. P. V. Nanosphere Lithography: Tunable Localized Surface Plasmon Resonance Spectra of Silver Nanoparticles. *J. Phys. Chem. B* **2000**, *104*, 10549–10556.
- Huang, X. H.; El-Sayed, I. H.; Qian, W.; El-Sayed, M. A. Cancer Cell Imaging and Photothermal Therapy in the Near-infrared Region by using Gold Nanorods. *J. Am. Chem. Soc.* **2006**, *128*, 2115–2120.
- Chen, X.; Zhu, H. Y.; Zhao, J. C.; Zheng, Z. F.; Gao, X. P. Visible-light-driven Oxidation of Organic Contaminants in Air with Gold Nanoparticle Catalysts on Oxide Supports. *Angew. Chem.* **2008**, *120*, 5433–5436; *Angew. Chem., Int. Ed.* **2008**, *47*, 5353–5356.
- Zheng, Y.; Chen, C.; Zhan, Y.; Lin, X.; Zheng, Q.; Wei, K.; Zhu, J. Photocatalytic Activity of Ag/ZnO Heterostructure Nanocatalyst: Correlation between Structure and Property. *J. Phys. Chem. C* **2008**, *112*, 10773–10777.
- Wang, Z. L.; Song, J. Piezoelectric Nanogenerators Based on Zinc Oxide Nanowire Arrays. *Science* **2006**, *312*, 242–246.

- (18) Manekthodi, A.; Lu, M. Y.; Wang, C. W.; Chen, L. J. Direct Growth of Aligned Zinc Oxide Nanorods on Paper Substrates for Low-Cost Flexible Electronics. *Adv. Mater.* **2010**, *22*, 4059–4063.
- (19) Wu, D.; Long, M. Realizing Visible-Light-Induced Self-Cleaning Property of Cotton through Coating N-TiO₂ Film and Loading AgI Particles. *ACS Appl. Mater. Interfaces* **2011**, *3*, 4770–4774.
- (20) Wu, D.; Wang, L.; Song, X.; Tan, Y. Enhancing the Visible-light-induced Photocatalytic Activity of the Self-cleaning TiO₂-coated Cotton by Loading Ag/AgCl Nanoparticles. *Thin Solid Films* **2013**, *540*, 36–40.
- (21) Wang, R. H.; Wang, X. W.; Xin, J. H. Advanced Visible-Light-Driven Self-Cleaning Cotton by Au/TiO₂/SiO₂ Photocatalysts. *ACS Appl. Mater. Interfaces* **2010**, *2*, 82–85.
- (22) Afzal, S.; Daoud, W. A.; Langford, S. J. Photostable Self-Cleaning Cotton by a Copper(II) Porphyrin/TiO₂ Visible-Light Photocatalytic System. *ACS Appl. Mater. Interfaces* **2013**, *5*, 4753–4759.
- (23) Khajavi, R.; Berendjchi, A. Effect of Dicarboxylic Acid Chain Length on the Self-Cleaning Property of Nano-TiO₂-Coated Cotton Fabrics. *ACS Appl. Mater. Interfaces* **2014**, *6*, 18795–18799.
- (24) Manna, J.; Rana, R. K. Oriented Morphogenesis of ZnO Nanostructures from Water-Soluble Zinc Salts under Environmentally Mild Conditions and Their Optical Properties. *Chem.—Eur. J.* **2012**, *18*, 498–506.
- (25) Manna, J.; Begum, G.; Kumar, K. P.; Misra, S.; Rana, R. K. Enabling Antibacterial Coating via Bioinspired Mineralization of Nanostructured ZnO on Fabrics under Mild Conditions. *ACS Appl. Mater. Interfaces* **2013**, *5*, 4457–4463.
- (26) Yao, K. S.; Wang, D. Y.; Ho, W. Y.; Yan, J. J.; Tzeng, K. C. Photocatalytic Bactericidal Effect of TiO₂ Thin Film on Plant Pathogens. *Surf. Coat. Technol.* **2007**, *201*, 6886.
- (27) Begum, G.; Manna, J.; Rana, R. K. Controlled Orientation in a Bio-Inspired Assembly of Ag/AgCl/ZnO Nanostructures Enables Enhancement in Visible-Light-Induced Photocatalytic Performance. *Chem.—Eur. J.* **2012**, *18*, 6847–6853.
- (28) Urrutia, A.; Rivero, P. J.; Ruete, L.; Goicoechea, J.; Matías, I. R.; Arregui, F. J. Single-stage in situ Synthesis of Silver Nanoparticles in Antibacterial Self-assembled Overlays. *Colloid Polym. Sci.* **2012**, *290*, 785–792.
- (29) Moussodia, R.-O.; Balan, L.; Merlin, C.; Mustin, C.; Schneider, R. Biocompatible and Stable ZnO Quantum Dots Generated by Functionalization with Siloxane-core PAMAM Dendrons. *J. Mater. Chem.* **2010**, *20*, 1147–1155.
- (30) Ramanathan, T.; Fisher, F. T.; Ruoff, R. S.; Brinson, L. C. Amino-Functionalized Carbon Nanotubes for Binding to Polymers and Biological Systems. *Chem. Mater.* **2005**, *17*, 1290–1295.
- (31) Zheng, Y.; Zheng, L.; Zhan, Y.; Lin, X.; Zheng, Q.; Wei, K. Ag/ZnO Heterostructure Nanocrystals: Synthesis, Characterization, and Photocatalysis. *Inorg. Chem.* **2007**, *46*, 6980–6986.
- (32) Zhang, M.; Wang, P.; Sun, H.; Wang, Z. Superhydrophobic Surface with Hierarchical Architecture and Bimetallic Composition for Enhanced Antibacterial Activity. *ACS Appl. Mater. Interfaces* **2014**, *6*, 22108–22115.
- (33) Prabhu, S.; Eldho, K. P. Silver Nanoparticles: Mechanism of Antimicrobial Action, Synthesis, Medical Applications, and Toxicity Effects. *Int. Nano Lett.* **2012**, *2*, 32.